Supporting Information

Structure and Absolute Configuration of Karlotoxin, an Ichthyotoxin from the Marine Dinoflagellate *Karlodinium veneficum*

Jiangnan Peng,[a] Allen R. Place,[b] Wesley Yoshida,[c] Clemens Anklin,[d] and Mark T. Hamann[a]

[a]*Department of Pharmacognosy and National Center for Natural Products Research, School of Pharmacy, University of Mississippi, MS 38677, USA.*

[b]*Center of Marine Biotechnology, University of Maryland Biotechnology Institute, Suite 236 Columbus Center, Baltimore, MD 21202, USA.*

[c]*Department of Chemistry, University of Hawaii at Manoa, HI 96822, USA*

[d]*Bruker BioSpin, 15 Fortune Drive, Billerica, MA 01821, USA*

^{1}H, ^{13}C, INADEQUATE, and HMBC Data for Karlotoxin-2 (KmTx2)

No.	δ_C	δ_H	INADEQUATE	HMBC	NOESY	ROESY
1a	66.90 CH_2	3.52 dd, 11.4, 4.2	C2	C-2, 3		H-3a,b
1b		3.46 dd, 11.4, 5.6		C-2, 3		H-3b w
2	73.23 CH	3.65 m	C1, 3	C-1, 3, 4	H-3a,b,	H-3a,b,
3a	37.73 CH_2	2.18 dt, 14.4, 6.6	C2, 4	C-1, 2, 4, 5	H-2	H-2, 1a, 5, 4
3b		2.29 dt 14.4, 6.6		C-1, 2, 4, 5	H-2	H-2, 1a, 5, 4
4	128.64 CH	5.69 dt 15.0, 7.2	C3, 5	C-2, 3, 5, 6		H-3a,b, 6
5	137.08 CH	5.54 dd 15.0, 7.2	C4, 6	C-3, 4, 6		H-6, 3a,b(w), 7 w
6	73.8 CH	4.02 m	C5, 7	C-4, 5, 7, 8		H-5, 4
7	38.48 CH_2	1.53 m	C6, 8	C-5, 8		
8a	22.96 CH_2	1.55 m	C7, 9			
8b		1.38 m				
9a	38.44 CH_2	1.50 m	C8, 10	C-8		
9b		1.46 m		C-8, 9, 11		
10	72.45 CH	3.55 m	C9, 11			H-12a, 11a, 9a
11a	38.56 CH_2	1.50 m	C10, 12			
11b		1.42 m		C-10		
12a	23.28 CH_2	1.62 m	C11, 12			
12b		1.41 m				
13	39.88 CH_2	1.48 m	C12, 14	C-14		
14	70.50 CH	3.65 m	C13, 15			H-15a, 64
15a	41.01 CH_2	1.67 m	C14, 16	C-14		H-14, 64
15b		1.27 m			H-17	H-17, 64, 16, 17
16	33.38 CH	1.98 m	C17, 15, 64			H-18, 17, 64, 15b
17	80.05 CH	3.14 dd 6.0, 4.2	C16, 18	C-15, 16, 64	H-19a, 15b	H-19a,b, 15b, 18, 16, 64
18	73.13 CH	3.62 m	C17, 19	C-19, 20	H-19a, 17w, 64	H-19a, 17, 16, 64
19a	32.67 CH_2	1.63 m	C18, 20	C-17	H-18, 17	H-17, 18
19b		1.55 m			H-22	H-22
20a	31.57 CH_2	1.61 m	C19, 21		H-22	H-22
20b		1.37 m				
21	35.08 CH	1.90 m	C20, 22, 65		H-22, 65	H-22, 23, 65
22	73.80 CH	3.69 dd, 9.0, 1.8	C21	C-20, 23, 24	H-23, 21, 20a	H-23, 21, 20a
23	74.07 CH	3.33 m	C25	C-21, 22, 25	H-65, 22	H-65, 22, 25b, 21, 25a w
24	71.68 CH	3.87 m	C23, 25		H-25a,b, 23	H-26b, 23, 22
25a	35.40 CH_2	1.69 m	C24, 26			
25b		1.52 m				
26a	24.52 CH_2	1.54 m	C25, 27		H-66	
26b		1.46 m				
27a	33.17 CH_2	1.70 m	C26, 28			
27b		1.28 m			H-29	H-29
28	36.52 CH	1.76 m	C27, 29, 66		H-29, 66	H-29, 66
29	80.18 CH	3.10 dd 7.2, 3.6	C28, 30	C-27, 28, 31, 66	H-30, 31a,b, 28, 27b, 66	H-30, 31a,b, 28, 27b, 66
30	68.57 CH	3.91 dt, 10.2, 1.7	C29	C-32	H-36, 29, 32, 31a,b, 66	H-36, 29, 32, 31a,b, 66

31a	34.67 CH_2	1.84 brt, 12.0	C32	C-32	H-29, 36, 33, 30	H-29, 36, 33, 30, 32
31b		1.70 m		C-30	H-32, 29, 33, 30, 36	H-32, 29, 33, 30, 36
32	74.72 CH	4.12 dt 10.8, 2.0	C31, 33	C-33, 34	H-30, 31b, 33	H-30, 31a,b, 33
33	73.17 CH	3.73 m	C32	C-34, 35	H-31a,b, 32	H-31a,b, 32
34	73.18 CH	3.73 m	C35	C-33, 35	H-36	H-36
35	71.04 CH	3.85 m	C34, 36	C-33, 34	H-38a	H-38a
36	78.12 CH	3.40 m	C35, 37	C-34, 35, 32, 37, 38	H-31a, 38b, 30, 37, 34	H-31a, 38b, 39a,b, 30, 37, 34
37	72.55 CH	4.02 m	C36, 38		H-38a, 39b, 36	H-38a, 39b, 36
38a	31.57 CH_2	2.04 m	C37, 39		H-67a, 37, 35	H-67a, 37, 35
38b		1.70 m		C-40	H-67a	H-67a, 36
39a	27.56 CH_2	2.45 m	C38	C-40	H-39b,	H-39b, 67a, 36, 41, 37w
39b		2.15 m		C-40	H-39a, 37	H-36, 37, 39a, 67a
40	151.40 C		C41, 67			
41	76.97 CH	4.23 d 9.0	C40, 42	C-39, 40, 42, 43	H-67b, 42	H-39a, 42, 43, 44a,b, 49, 51
42	75.04 CH	3.39 brd 8.4	C41, 43	C-40, 41, 44	H-41, 43, 44a, b	H-41, 43, 44a, b, 67b
43	70.40 CH	4.06 m	C42, 44	C-44	H-42, 49	H-42, 49
44a	31.57 CH_2	2.12 m	C43, 45	C-45, 46	H-42	H-41
44b		1.58 m		C-45, 46	H-42, 43	H-42, 43, 41
45	67.36 CH	4.07 m	C44, 46	C-44	H-48	H-48
46	68.72 CH	4.05 m	C45, 47	C-44, 45	H-47	H-47
47	80.70 CH	3.74 brd 10.4	C46, 48	C-43, 45, 46, 48, 49	H-46	H-46, 49
48	71.90 CH	3.99 dd 10.2, 2.4	C47, 49	C-46, 47, 49, 50	H-45, 47, 49	H-45, 49
49	74.28 CH	4.39 dd 7.2, 3.0	C48, 50	C-50, 51	H-45, 43, 41	H-41, 43, 48, 47, 50, 51
50	128.51 CH	5.61 dd 15.0, 7.2	C49, 51	C-52	H-49 weak	H-47, 49, 52
51	136.15 CH	5.81 dt 15.0, 7.2	C50, 52	C-49, 52, 53	H-49 weak	H-49, 52, 41
52	33.83 CH_2	2.11 m	C51, 53	C-50, 51, 53		H-50, 51
53	30.62 CH_2	1.44 m	C53			
54	30.50 CH_2	1.34 m				
55	30.54 CH_2	1.34 m				
56	30.72 CH_2	1.34 m				
57	30.80 CH_2	1.34 m				
58	30.43 CH_2	1.42 m	C59			
59	33.83 CH_2	2.11 m	C58, 60	C-58, 60, 61		
60	137.31 CH	5.75 dt 15.0, 7.2	C59, 61	C-58, 59, 62		
61	127.67 CH	6.05 dd, 15.0, 10.8	C60, 62	C-59, 62, 63		
62	135.35 CH	6.45 dd 13.2, 10.8	C61, 63	C-60, 61, 63		
63	119.57 CH	6.23 d 13.2	C62	C-61, 62		
64	17.59 CH_3	0.99 7.2	C16	C-15, 16, 17	H-18	H-18
65	13.39 CH_3	0.93 d, 7.2	C21	C-20, 21, 22	H-20a, 23	H-23, 20a
66	16.87 CH_3	0.98d, 7.8	C28	C-27, 28, 29	H-29, 30, 25b or 26a	H-29, 30, 27b
67a	113.56 CH_2	5.03 s	C40	C-39, 40, 41	H-38a,b	H-39a,b, 38a,b
67b		5.08 s		C-39, 41	H-41	H-42, 41

600 MHz for proton, 125 MHz for carbon, in CD3OD. w: weak correlation

1. Experiments Section

General Experiments. High-resolution mass spectrometry data was obtained on a Bruker MicroTOF mass spectrometer. ^{1}H, ^{13}C, DEPT, COSY, HSQC, HMBC, NOESY, ROESY, TOCSY, and 2D INADEQUATE spectra of 1.3 mg of approximately 10% uniform ^{13}C metabolite were measured on a Bruker Avance 600 MHz NMR equipped with a 3 mm carbon cryo-probe. HETLOC, HSQMBC, 1D TOCSY with decoupling were measured on a Varian 500 MHz NMR. The NMR of the degradation products were recorded using a 1 mm probe on Bruker 500 MHz NMR. All organic solvents and water used were of HPLC grade or better and were purchased from Burdick & Jackson. Syringe filters PFTE (13 mm diameter, 0.2 μm pore size) and GF/F (13 mm diameter, 1 μm pore size) filters were obtained from Whatman. Final purification was accomplished using C18 and NH2 bonded stationary phases.

Culturing

K. veneficum strain CCMP 2064 was acquired from the Center for the Culture of Marine Phytoplankton (CCMP). The strain was isolated in November 1998 from a fish-kill on the Wilmington River, Georgia and deposited on May 3, 2003. The strain is unialgal but not axenic and was cultured phototrophically in 15 psu filtered (0.22 μm) natural seawater combined with f/2 nutrients and vitamins without Si[1] at 100 μEinstein m^{-2} s^{-1} and 20 °C ambient temperature.[1] Cell densities were measured using a Coulter Multisizer II (Beckman-Coulter) counter and cells ml^{-1} determined using Accucomp (Version 2.01) software.

Toxin isolation

To obtain adequate quantities of toxin for structural characterization, 5.8 $x10^{9}$ cells

(40 L of culture) were grown with $NaH^{13}CO_3$ (50 mg/L) for 28 days, filtered onto 125 mm GF/F filters (Whatman), and the toxin (>95% of recovered material) from the filtrate was concentrated on three 55g C18 columns (AnaLogix, Sorbtech Technologies) in parallel. Extraction of the cells with MeOH only provided 5% of the recovered toxin. The columns had been activated by passing 200 mL methanol followed by 200 mL HPLC-grade water through each column. Toxin was eluted using 200 mL methanol:water as described above for smaller columns, except that the 60% and 80% methanol fractions were collected, pooled and dried under vacuum at 40 °C. The concentrated toxin from the pooled 60-80% C18 eluent was then purified using reverse phase chromatography on a semipreparative scale C18 column (Phenomenex Hyperprep HS C18-80S, 250 X 10 mm, 5 µ), at a flow rate of 4 mL min^{-1}. Fractions corresponding to KmTx 2 were collected using a fraction collector (61364A, AFC, Agilent) based on known retention times. Fractions with the same elution times were pooled and dried under vacuum and resuspended in methanol:H_2O (80:20). From the total 40 L, 2.5 mg of enriched material was obtained.

Known aliquots of the purified toxins were placed onto a tared aluminum weigh boat in triplicate, dried at 60 °C overnight and weighed the following day on a Mettler UMT2 microgram balance. The A_{235} was 3.554 X 10^5.

2 Structure Elucidation

2.1 Assembly of the Carbon Skeleton

Most carbon connections were established using 2D INADEQUATE experiments (see Figure S1). The connection between carbons absent of INADEQUATE correlations

and the two pyran rings were achieved in addition to validation of the structure by hetero-nuclear correlations in the HMBC experiments (see Figure S2).

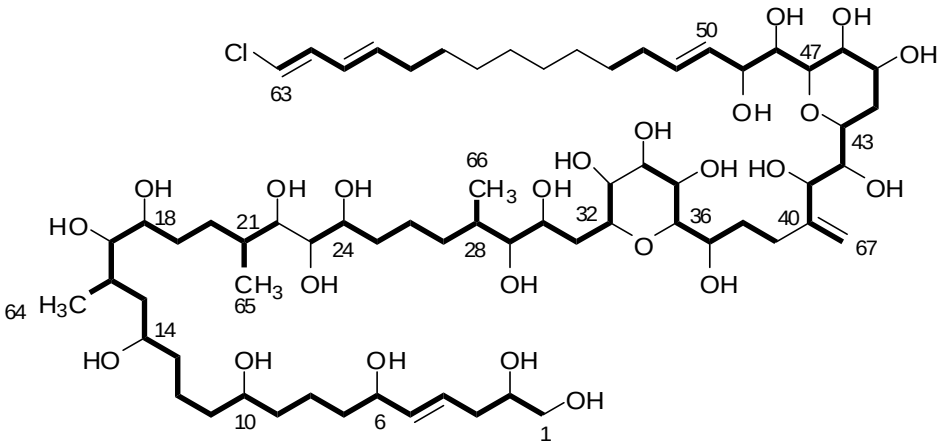

Figure S1. Structure of karlotoxin-2. Bold shows the INADEQUATE connections.

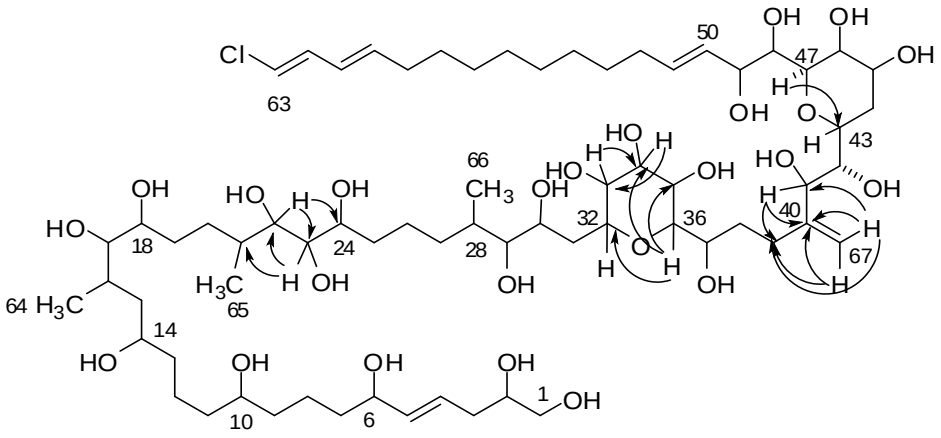

Figure S2. Key HMBC Correlations

2.2 Determination of the Relative Configuration

2.2.1 Configuration of C36~C49

C47~C49 and C41~C43: The relative configuration of C49-C48 was determined effectively by $^{3}J_{H,H}$ and $^{2,3}J_{C,H}$. The small ^{3}J(H49, H48) value indicated the Gauche relationship of this two protons (see Figure 3). The small two bond hetero-nuclear coupling constants between H-49/C48 and H48/C49 suggested that the H49/C48-OH and

H48/C49-OH assume an anti-orientation. This is confirmed by the small three bond hetero-nuclear coupling constants between H-49/C47 and H48/C50. The large coupling constant between H48 and H47 indicated the anti orientation of these two protons, in which situation NOE is required for the determination of the relative configuration. An NOE correlation between H49 and H43 revealed the *erythro* relationship of C48 and C47 (see Figure S3). Similarly, the configuration of C43~C41 was established as depicted in Figure 3.

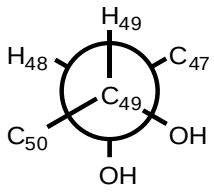

$^{3}J_{(H\text{-}49,\ H\text{-}48)}$ 3.0
$^{3}J_{(H\text{-}49,\ C\text{-}47)}$ 0.0
$^{3}J_{(C\text{-}50,\ H\text{-}48)}$ 3.5
$^{2}J_{(C\text{-}49,\ H\text{-}48)}$ 1.5
$^{2}J_{(C\text{-}48,\ H\text{-}49)}$ small*

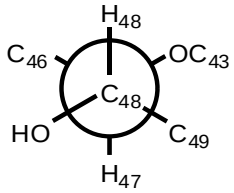

$^{3}J_{(H\text{-}48,\ H\text{-}47)}$ 10.4
$^{2}J_{(C\text{-}48,\ H\text{-}47)}$ -5.7
$^{2}J_{(C\text{-}47,\ H\text{-}48)}$ -3.6
NOE H-49/H-43

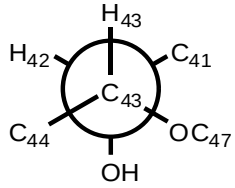

$^{3}J_{(H\text{-}43,\ H\text{-}42)}$ small
$^{3}J_{(H\text{-}42,\ C\text{-}44)}$ small#
$^{3}J_{(C\text{-}41,\ H\text{-}43)}$ small*
$^{2}J_{(C\text{-}43,\ H\text{-}42)}$ small*
$^{2}J_{(C\text{-}42,\ H\text{-}43)}$ small*

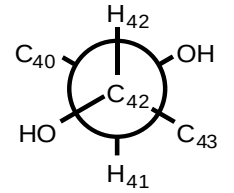

$^{3}J_{(H\text{-}42,\ H\text{-}41)}$ 9.0
$^{2}J_{(C\text{-}42,\ H\text{-}41)}$ -5.2
$^{2}J_{(C\text{-}41,\ H\text{-}42)}$ -4.3
NOE H-43/41-OH
(in DMF)

Figure S3. Coupling constants and Configuration of C41~C43 and C47~C49

Configuration of the two Pyran Rings: The NOE correlation between H43 and H49 suggested *axial* orientation for both H43 and C48, and equatorial orientation for H47. The appearance of H44a (δ 2.12, brq, J = 11.9 Hz) in a 1D TOCSY spectrum indicated

large coupling constants for H44a/H43 and H44a/H45, revealing the axial orientation of H43, H44a, and H45. Finally, an NOE between H47/H46 and no NOE between H44a/H46 suggested an equatorial H46. Thus the relative configuration of C43~C47 pyran ring was defined as shown in Figure S4.

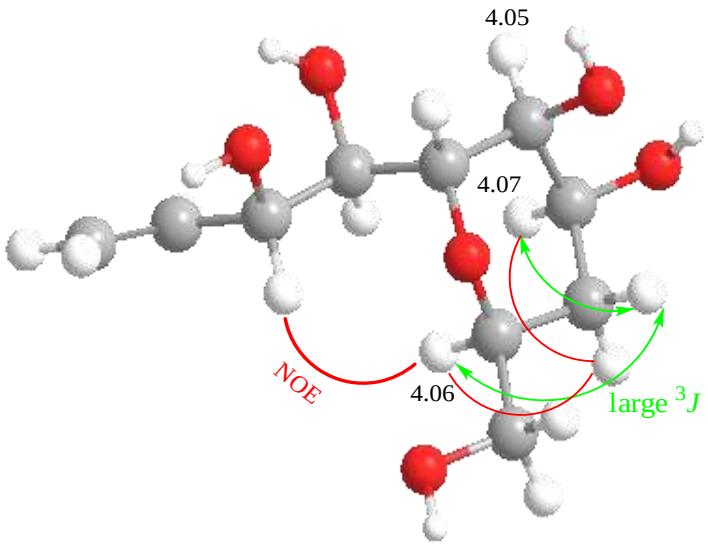

Figure S4. Configuration of C43-C47. Red represents NOE and green for large $^3J_{H,H}$

The configuration of the second pyran ring C32-C36 was established in a similar way (see Figure S5). NOE correlations between H36/H31a and H36/H32 indicated the axial orientation of H36 and C31. The appearance of H35 (δ 3.85, dd, J = 7.6, 7.6 Hz) in a 1D TOCSY spectrum suggested that H35 and H34 were axial protons. The excitation of H32 (δ 4.12, dt, J = 11.4, 2.6 Hz) resulted in the enhancement of H33 (δ 3.73, brd, J = 2.6 Hz) in a 1D ROESY spectrum.

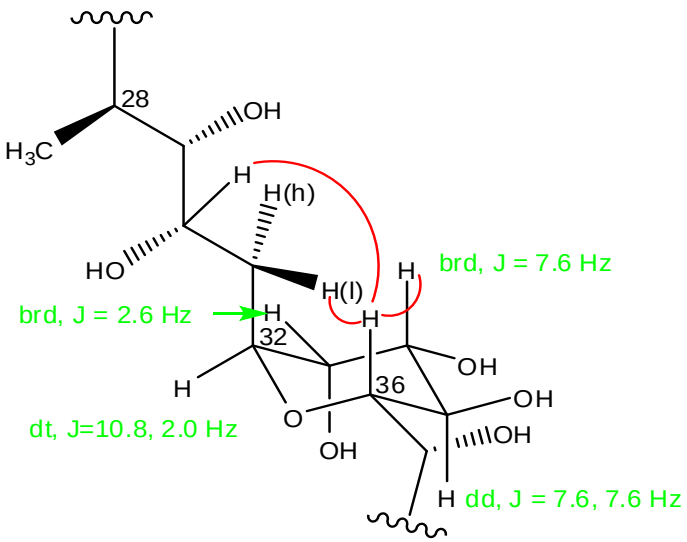

Figure S5. Configuration of C32-C36. Red indicated NOE correlations.

Configuration of C37~C41. To correlate the configuration of the two rings, the diastereomeric relationship between C37 and C41 had to be established. This was achieved by $^{3}J_{H,H}$, $^{2,3}J_{C,H}$, and NOE data (Figure S6). The prominent NOE correlations between H67(H) and the two protons at C38 revealed that C67 is syn to C38. The $^{3}J_{H,H}$ values of H37~H39 indicated the zigzag conformation of C37~C40 and assigned the diastereotopic methylene protons as shown in Figure 6. The anti orientation of H41 and C39 was determined by a large ^{3}J(H41, C39) and a intense NOE between H-41 and H67(L). The orientation of C42 and C39 was determined by a strong NOE between H42 and H39(H).

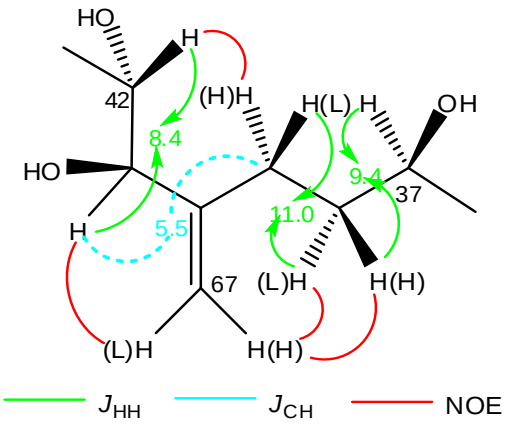

Figure S6. Relative configuration of C37~C41

Configuration of C36~C37 and C28~C32.

The intermediate coupling constant between H36 and H37 indicated the presence of two alternating conformers, which represent gauche or anti orientation of H36/H37.[12] The gauche orientation of H36/C38 was suggested by the small ^{3}J(H36, C38), while H37/C35 and H36/C37-OH were gauche or anti orientation suggested by the intermediate ^{2}J(H, C). This fits the configuration and conformation shown in Figure 7. Similarly, H28 and H29 showed an intermediate coupling constant and the relative configuration between C28 and C29 assigned as shown in Figure S7.

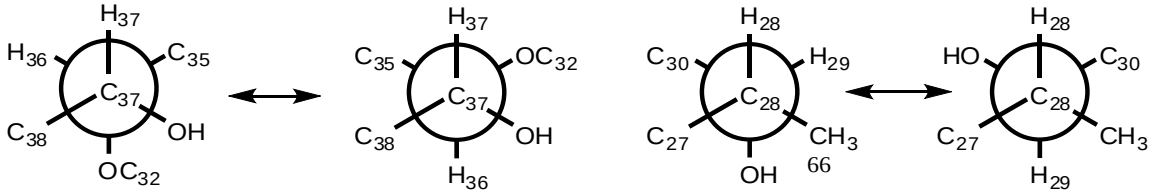

$^{3}J_{(H\text{-}37,\ H\text{-}36)}$	5.5l
$^{3}J_{(C\text{-}38,\ H\text{-}36)}$	small#
$^{2}J_{(C\text{-}37,\ H\text{-}36)}$	-3.2
$^{2}J_{(C\text{-}36,\ H\text{-}37)}$	-2.7

$^{3}J_{(H\text{-}29,\ H\text{-}28)}$	7.3
$^{3}J_{(C\text{-}66,\ H\text{-}29)}$	2.0
$^{2}J_{(C\text{-}29,\ H\text{-}28)}$	-4.6

Figure S7. Relative configuration of C28~C29 and C36~C37

The configuration of C30 and C32 was correlated by assignment of the diastereomeric methylene protons of C31 (Figure S8). The gauche and anti relationship of H31(H)/H32 and H31(L)/H32 were indicated by the small and large coupling constants between H313(H)/H32 and H31(L)/H32, respectively. The anti orientation of H31(H)/C32-O was determined by the small ^{2}J(H31H, C32), while the gauche orientation for H32/C30 and H31(L)/C32-O were assigned by the small ^{3}J(H32, C30) and large ^{2}J(H31L, C32) (see Figure 8). H31(L) was determined to be gauche with H30 and anti to C30-OH by the small ^{3}J(H31L, H30) and ^{2}J(H32L, C34). H33(H) was indicated as anti to H34 by the large ^{3}J(H33H, H34). The relative configuration of C30/C29 was determined to be *threo* by the gauche orientation of H30/H29 indicated by small coupling constant of H30/H29 and the anti orientation of H30/C29-OH and H29/C30-OH deduced by small ^{2}J(H29, C30) and ^{2}J(H30, C29). Thus, the relative configuration of C29~C32 was determined as shown in Figure S8.

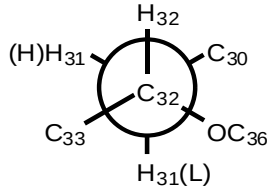

$^{3}J_{(H\text{-}32,\ H\text{-}31H)}$ 2.6
$^{3}J_{(H\text{-}32,\ H\text{-}31L)}$ 11.4
$^{3}J_{(C\text{-}30,\ H\text{-}32)}$ 2.7
$^{2}J_{(C\text{-}32,\ H\text{-}31H)}$ -0.7
$^{2}J_{(C\text{-}32,\ H\text{-}31L)}$ -6.6

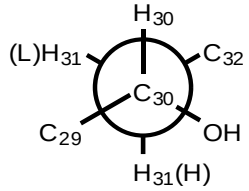

$^{3}J_{(H\text{-}30,\ H\text{-}31H)}$ 10.3
$^{3}J_{(H\text{-}30,\ H\text{-}31L)}$ 2.3
$^{3}J_{(C\text{-}32,\ H\text{-}30)}$ 2.5
$^{2}J_{(C\text{-}30,\ H\text{-}31H)}$ -5.8
$^{2}J_{(C\text{-}30,\ H\text{-}31L)}$ -0.8

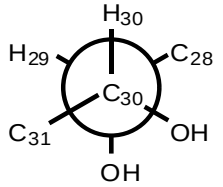

$^{3}J_{(H\text{-}30,\ H\text{-}29)}$ 3.1
$^{3}J_{(C\text{-}28,\ H\text{-}30)}$ small*
$^{2}J_{(C\text{-}30,\ H\text{-}29)}$ -0.5
$^{2}J_{(C\text{-}29,\ H\text{-}30)}$ -0.5

Figure S8. Configuration of C29~C32

2.2.2 Configuration of C21~C24

The gauche relationships of H23/H24 and H23/C25 were suggested by the small ^{3}J(H23, H24) and ^{3}J(H23, C25). H23 was determined to be anti to C24-OH by small ^{2}J(H23, C24). In addition, C22 is determined to be gauche to H24 by the NOE between H24 and H22, establishing the relative configuration of C23/C24. H23 was suggested to be anti to H22 by the large ^{3}J(H23, H22). The NOE between H-21and C23-OH and the large coupling constants of ^{2}J(H23, C22) and ^{2}J(H22, H23) determined the configuration of C23/C22. The relative configuration of C21/C22 was determined by small ^{3}J(H22, H21) and ^{3}J(C20, H22), large ^{3}J(C65, H22), and NOEs for H23/H65,21.

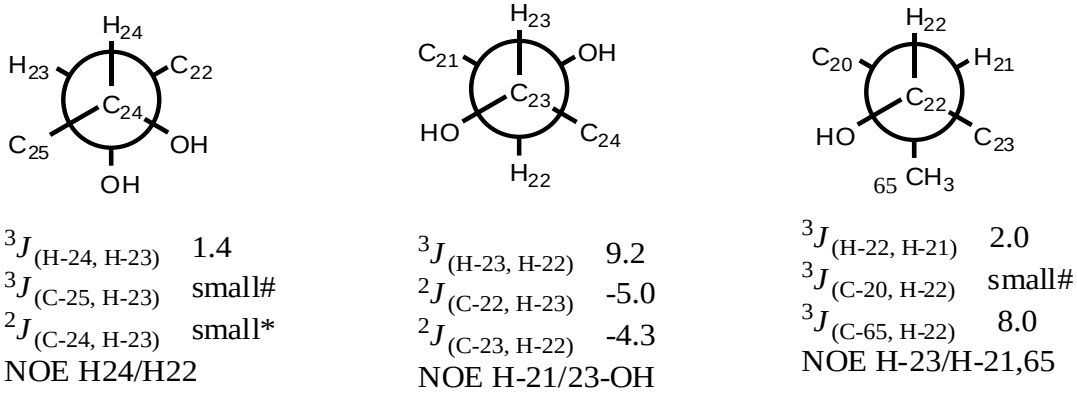

$^{3}J_{(H\text{-}24,\ H\text{-}23)}$ 1.4
$^{3}J_{(C\text{-}25,\ H\text{-}23)}$ small#
$^{2}J_{(C\text{-}24,\ H\text{-}23)}$ small*
NOE H24/H22

$^{3}J_{(H\text{-}23,\ H\text{-}22)}$ 9.2
$^{2}J_{(C\text{-}22,\ H\text{-}23)}$ -5.0
$^{2}J_{(C\text{-}23,\ H\text{-}22)}$ -4.3
NOE H-21/23-OH

$^{3}J_{(H\text{-}22,\ H\text{-}21)}$ 2.0
$^{3}J_{(C\text{-}20,\ H\text{-}22)}$ small#
$^{3}J_{(C\text{-}65,\ H\text{-}22)}$ 8.0
NOE H-23/H-21,65

Figure S9. Configuration of C21~C24

2.2.3 Configuration of C14~C18

The intermediate coupling constants between H18/H17 and H17/H16 suggested two alternative conformations for both C18/C17 and C17/C16. The small ^{3}J(H17, C19) and ^{3}J(H17, C64) indicated that both H17/C19 and H17/C64 are gauche in orientation. The ^{2}J(H17, C18), ^{2}J(H18, C17), and ^{2}J(H16, C17) showed intermediate coupling interactions between gauche and anti orientation. Thus, the configuration of C18~C16 was determined as shown in Figure S10.

The configuration of C14 was correlated to C16 through the assignment of the two diastereotopic methylene protons of C15. The anti-orientations of H15(H)/H16 and H15(L)/H14 were assigned by large ^{3}J(H15H, H16) and ^{3}J(H15L, H14), while gauche orientations of H15(L)/H16 and H15(H)/H14 were assigned by the small ^{3}J(H15L, H16) and ^{3}J(H15H, H14). The anti orientation of H15L/C64 and H15H/C14-OH were determined by large ^{3}J(H15L, C64) and small ^{2}J(H15H, C14).

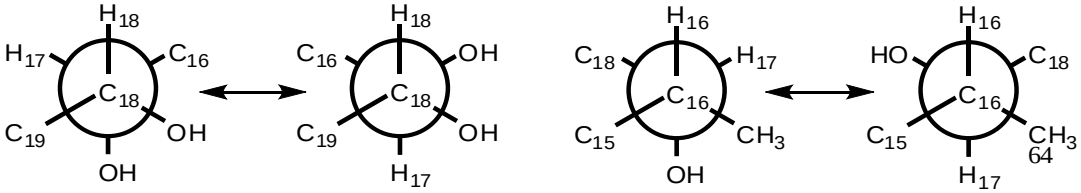

$^{3}J_{(H\text{-}18,\ H\text{-}17)}$	4.2
$^{3}J_{(C\text{-}19,\ H\text{-}17)}$	small*
$^{2}J_{(C\text{-}18,\ H\text{-}17)}$	-1.4
$^{2}J_{(C\text{-}17,\ H\text{-}18)}$	-1.8

$^{3}J_{(H\text{-}17,\ H\text{-}16)}$	6.3
$^{3}J_{(C\text{-}64,\ H\text{-}17)}$	1.5
$^{2}J_{(C\text{-}17,\ H\text{-}16)}$	-3.0

$^{3}J_{(H\text{-}16,\ H\text{-}15H)}$	10.7
$^{3}J_{(H\text{-}16,\ H\text{-}15L)}$	3.3
$^{3}J_{(C\text{-}64,\ H\text{-}15H)}$	3.1
$^{3}J_{(C\text{-}64,\ H\text{-}15L)}$	6.2

$^{3}J_{(H\text{-}14,\ H\text{-}15H)}$	3.3
$^{3}J_{(H\text{-}14,\ H\text{-}15L)}$	9.7
$^{2}J_{(C\text{-}14,\ H\text{-}15H)}$	-1.6
$^{2}J_{(C\text{-}14,\ H\text{-}15L)}$	-5.4

Figure S10. Configuration of C14~C18

2.3 Determination of the Absolute Configuration

2.3.1 Periodate degradation.

Karlotoxin-2 (1.7 mg) was dissolved in 1 mL of 0.1 M HIO_4 and stirred at room temperature for 40 min. After the solution was cooled to 0 ^{o}C, excess amount of $NaBH_4$ was added and kept for 1 hr. The reaction solution was loaded to a C8 cartridge column

(Phenomenex Strata, 5 g) and washed with 10 mL of H_2O followed by 10 mL of MeOH. The MeOH eluent was split in two fractions. Each fraction was dissolved in 2 mL of methylene chloride after removing of MeOH. (*R*)- or (*S*)-MPA (11 mg), EDC HCl (16 mg), and catalytic amount of DMAP were added and stirred overnight. The reaction solution was then pass through a 1 g silica gel SPE column and eluted with hexans:ethyl acetate 8:2. The eluent was separated on an analytical HPLC silica gel column to furnish **2b**/**2c**, **3b**/**3c**, and **4b**/**4c.** ^{1}H and COSY NMR spectra of each product were measured using a Bruker 1 mm probe. The chemical shifts differences between (*R*)- and (*S*)-MPA were determined and showed in Figure S11. The absolute configuration of C6, C10, C14, C21, and C28 were assigned as *R*, *R*, *S*, *S*, and *R*, respectively.

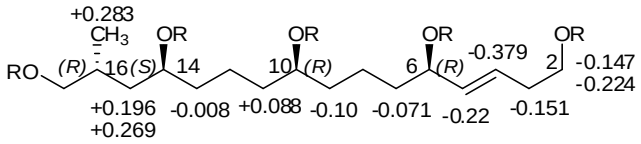

2b: R=(*R*)-MPA
2c: R=(*S*)-MPA

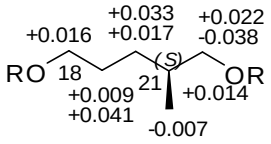

3b: R=(*R*)-MPA
3c: R=(*S*)-MPA

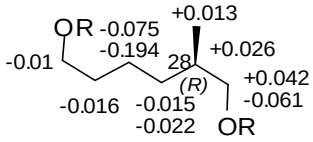

4b: R=(*R*)-MPA
4c: R=(*S*)-MPA

Figure S11. Chemical shifts differences between **2b**/**2c, 3b**/**3c**, and **4b**/**4c**

2.3.2 Synthesis of **3b**/**3c**, **4b**/**4c,** and **5b**/**5c**

3b/**3c.** A solution of (S)-dimethyl 2-methylpentanedioate (90 mg) in 4 mL of ether was treated with excess of $LiAlH_4$ (70 mg) at room temperature for 5 hr. The reaction mixture was then passed through a short silica gel column and eluted with MeOH:$CHCl_3$ (8:2, v/v) to yield (*S*)-2-methylpentane-1,5-diol (**3a**, 30 mg). **3a** was split in two fractions and esterified with (*R*)- or (*S*)-MPA as previous described to yield **3b** and **3c**. The proton NMR spectra of **3b** and **3c** from the degradation products of karlotoxin-2 and that from the synthesized material match very well (see Figure S12 and S13).

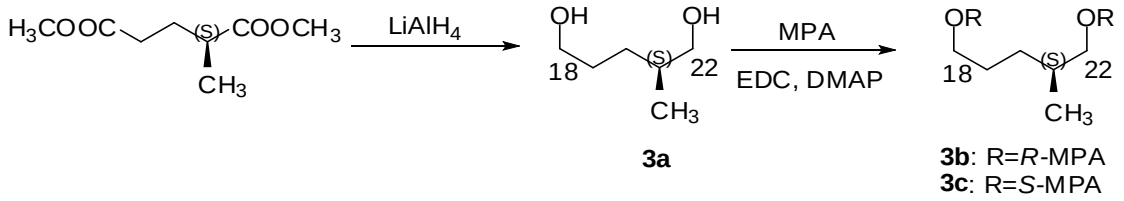

3a

3b: R=*R*-MPA
3c: R=*S*-MPA

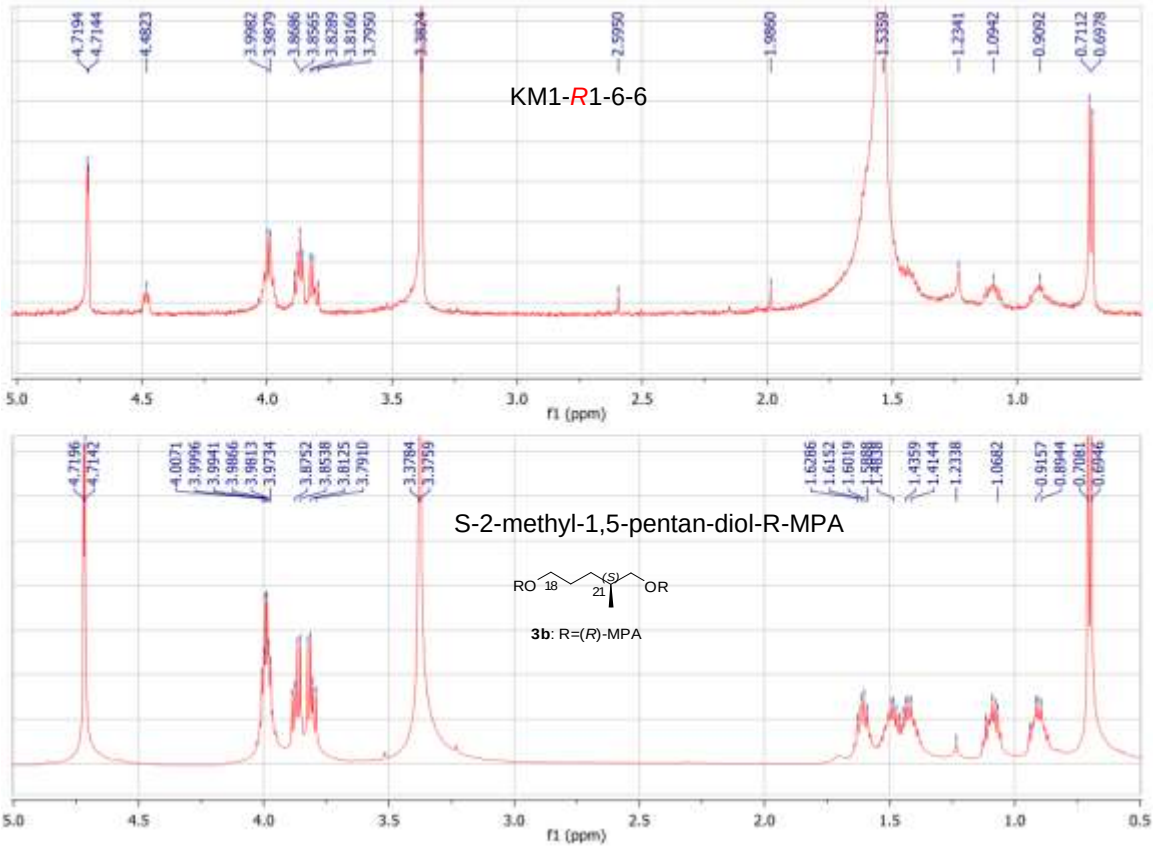

Figure S12. Proton NMR comparison of synthesized of **3b** and **3b** from degradation of karlotoxin-2

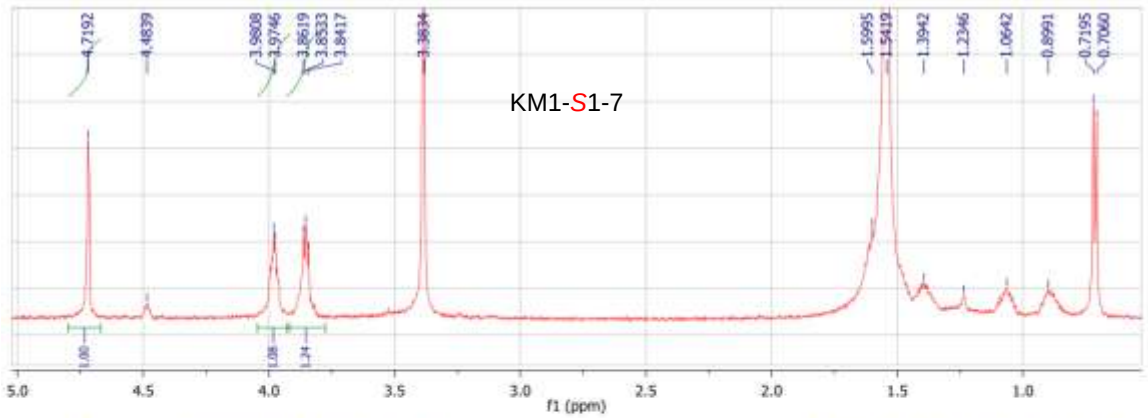

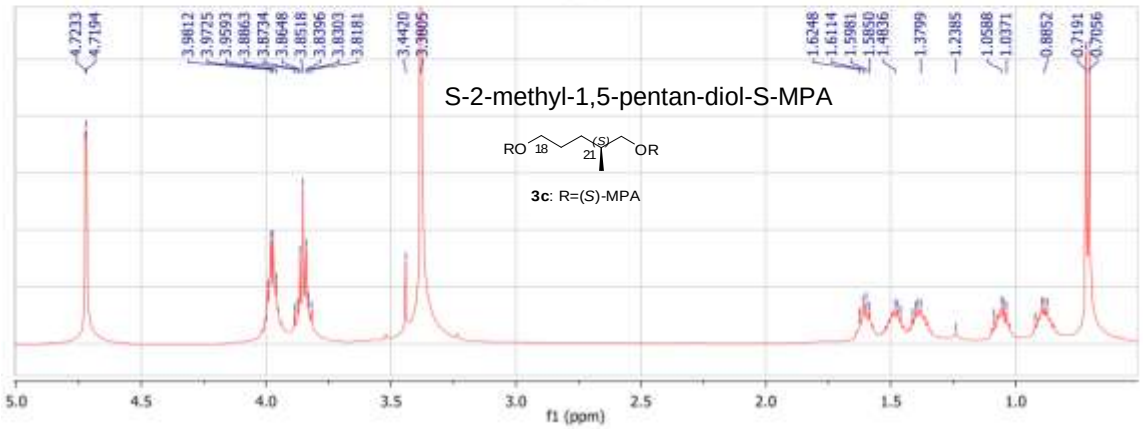

Figure S13. Proton NMR comparison of synthesized of **3c** and **3c** from degradation of karlotoxin-2

4b/**4c.** (*R*)-2-Methylhexane-1,6-diol (**4a**) and its isomer (*R*)-3-methylhexane-1,6-diol (**4a'**) were sysnthesized from (*R*)-3-methylcyclohexanone (bought from Aldrich) according to literature.[12] Separation of **4a**/**4a'** or their MPA esters **4b**/**4b'** and **4c**/**4c'** were not reached. The ^{1}H NMR data of **4b**, **4b'**, **4c**, **4c'** were readily assigned from **4b**/**4b'** and **4c**/**4c'** mixtures using 2D COSY and TOCSY spectra. The proton signals for methyl and hydroxylmethylene of **4b**/**4b'** and **4c**/**4c'** were separated. The ratios of **4b**/**4b'** and **4c**/**4c'** are about 2:1 based on the proton NMR (see Figure S14 and S15). The proton NMR

spectra of the degradation products **4b** and **4c** match with the synthesized **4b** and **4c** very well, especially for the characteristic signals of hydroxylmethylene (see Figure S14 and S15). These data clearly indicated the *R* configuration for C28.

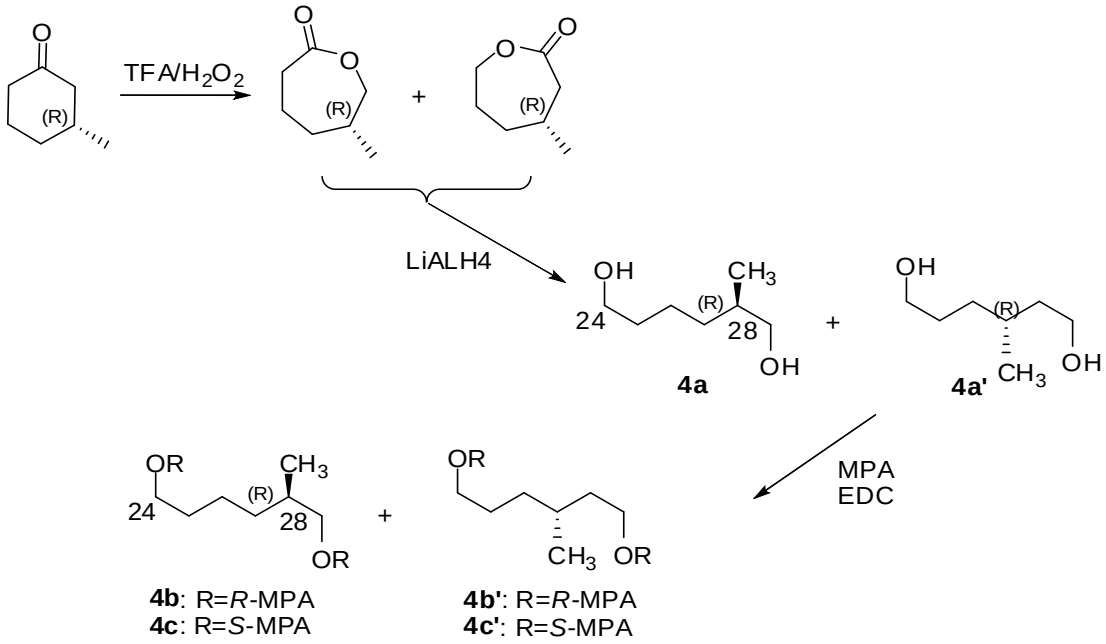

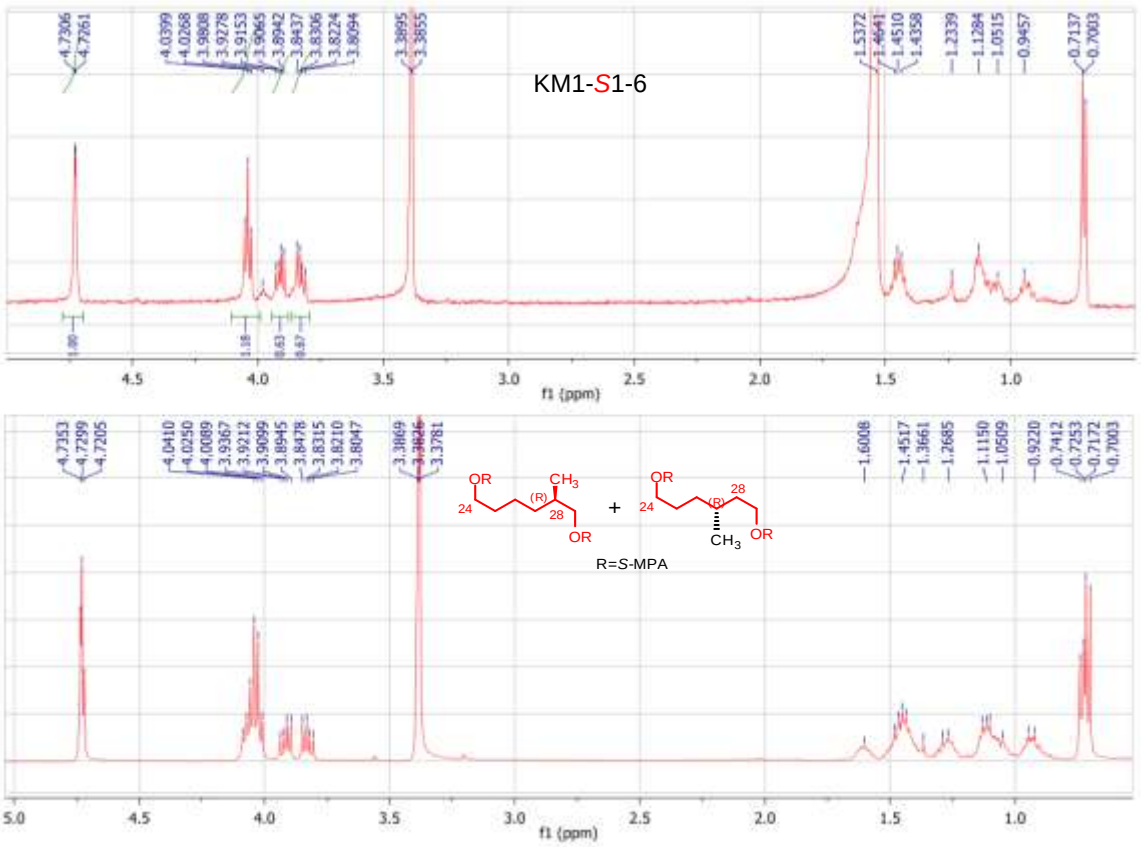

Figure S14. Proton NMR comparison of synthesized of **4c** and **4c** from degradation of karlotoxin-2

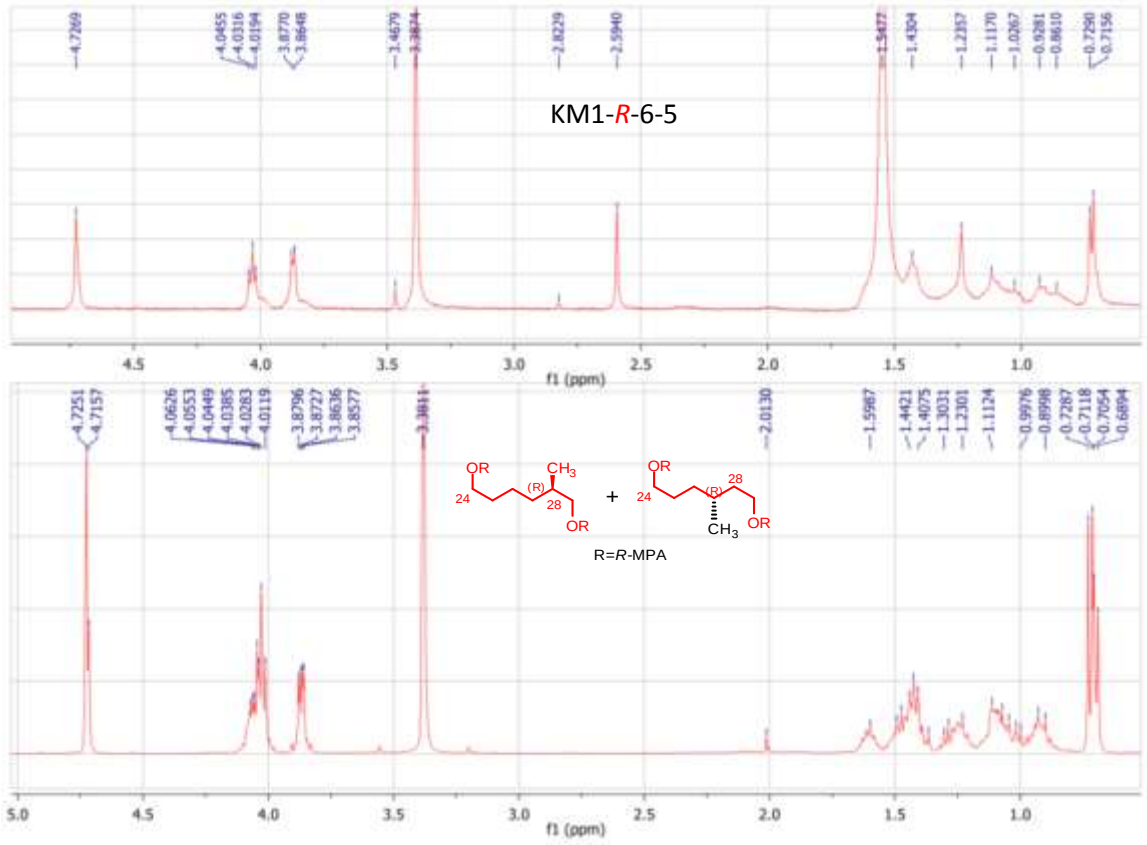

Figure S15. Proton NMR comparison of synthesized of **4b** and **4b** from degradation of karlotoxin-2

The absolute configuration of C32~C49 was determined by correlation with C28, which is opposite to that of amphidinol 3. The absolute configuration of C32~C49 of amphidinol 3 was determined on the correlation with C37, whose absolute configuration was deduced from Mosher's esters of the C31~C48 unit of the HIO_4 degradation products.[13] The crowd hydroxyl group (31, 33, 34, and 37) and as a results, the crowd MTPA esters in this degradation subunit (C31~C48), may affect the correct predict of the absolute configuration of C37 of amphidinol 3. The unusual large Δδ (H-38 - 0.57, H-40 +0.37, H-41 +0.30/0.37, H-70 +0.33/0.42) indicated an unusual conformation for this Mosher's ester.

5a/**5b.** (*R*)-Pent-4-ene-1,2-diol (**5a**) and (*S*)-Pent-4-ene-1,2-diol (**5b**) was synthesized from (*S*)-glycidol and (*R*)-glycidol, respectively, according to the literature.[2]

2.3.3 Olefin metathesis of KmTx 2

Grubbs' II catalyst (1.1 mg) was dissolved in 1 mL of methylenechloride and was flashed using ethylene stream. 100 μL of the Grubbs' catalyst solution was mixed with 100 μL of KmTx 2 (0.1 mg) in MeOH. The mixture was sealed in a round bottom flask. After flash the solution with ethylene, the mixture was stirred at room temperature under ethylene atmosphere for 24 hr. The reaction solution was filtered and checked by GC/MS equipped with chiral capillary column (Varian Chirasil DEX CB, 0.2 mm x 25 m). The product showed the retention time with (*R*)-Pent-4-ene-1,2-diol (**5a**). The mixture of the product and (*R*)-Pent-4-ene-1,2-diol (**5a**) showed one peak, while the mixture of the product with (*S*)-Pent-4-ene-1,2-diol (**5b**) showed two peaks (see Figure S-16), which indicated the R configuration for C2 of karlotoxin. A sample of amphodinol 3 kindly provided by Professor Michio Murata was processed using the method. The results (Figure S16 e-f) verified the revised configuration for C2 of amphodinol 3 and proved that karlatoxin and amphodinol 3 share the same *R* configuration for C2.

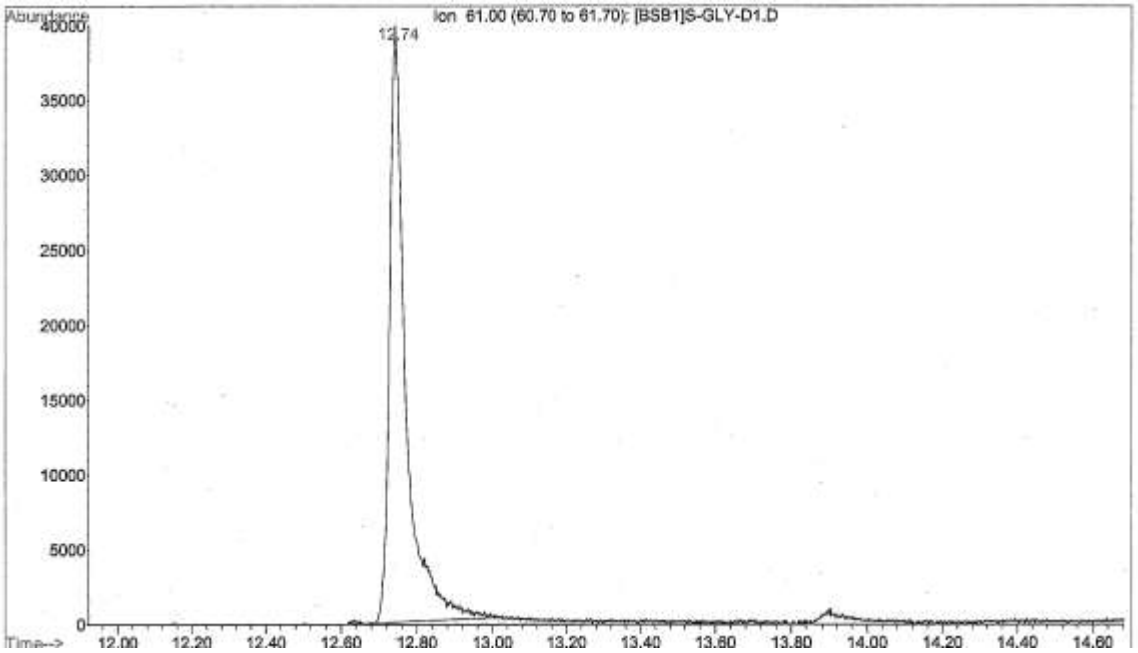

a. GC/MS of (*R*)-Pent-4-ene-1,2-diol (**5a**)

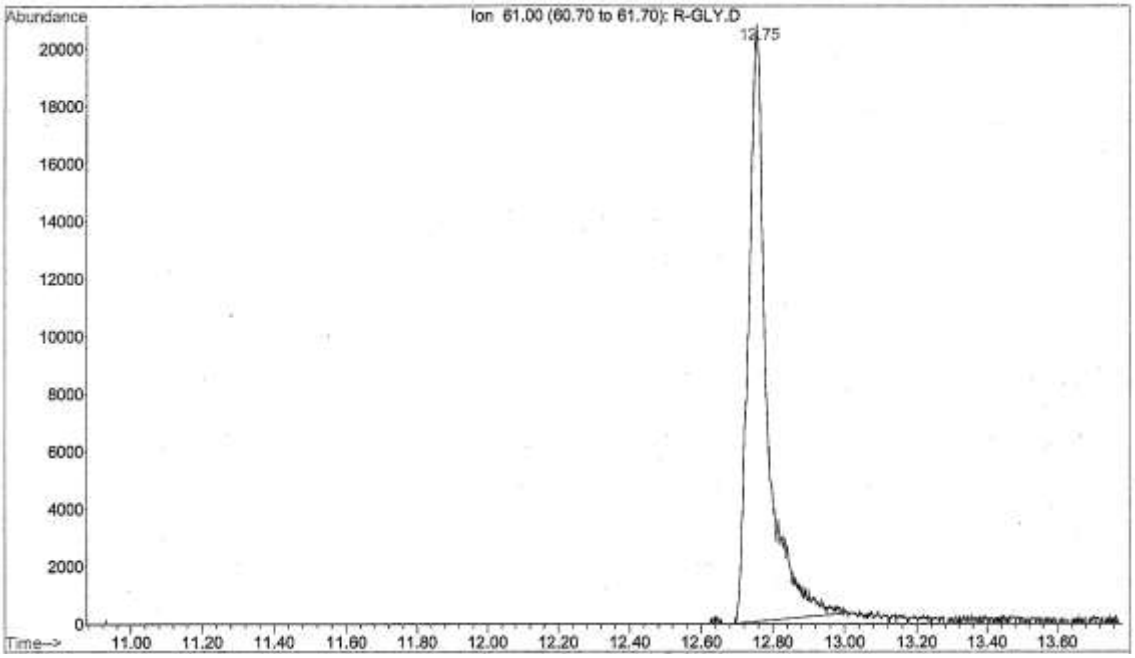

b. GC/MS of (*S*)-Pent-4-ene-1,2-diol (**5b**)

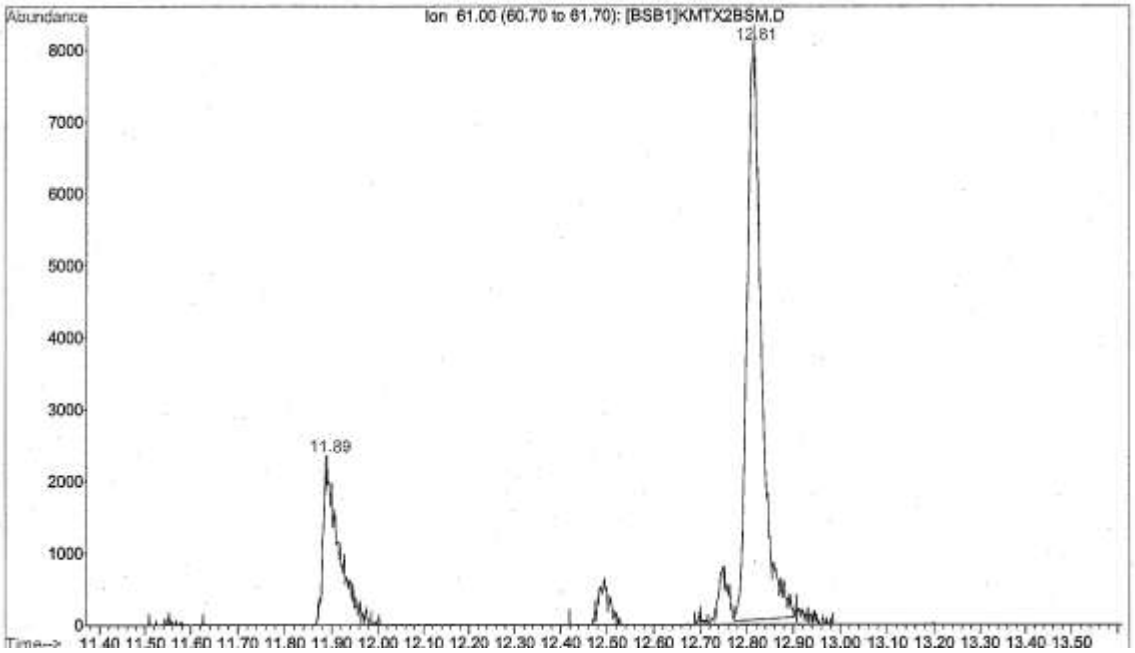

c. GC/MS of the mixture of KmTx2 Grubbs' metathesis products and (*R*)-Pent-4-ene-1,2-diol (**5a**)

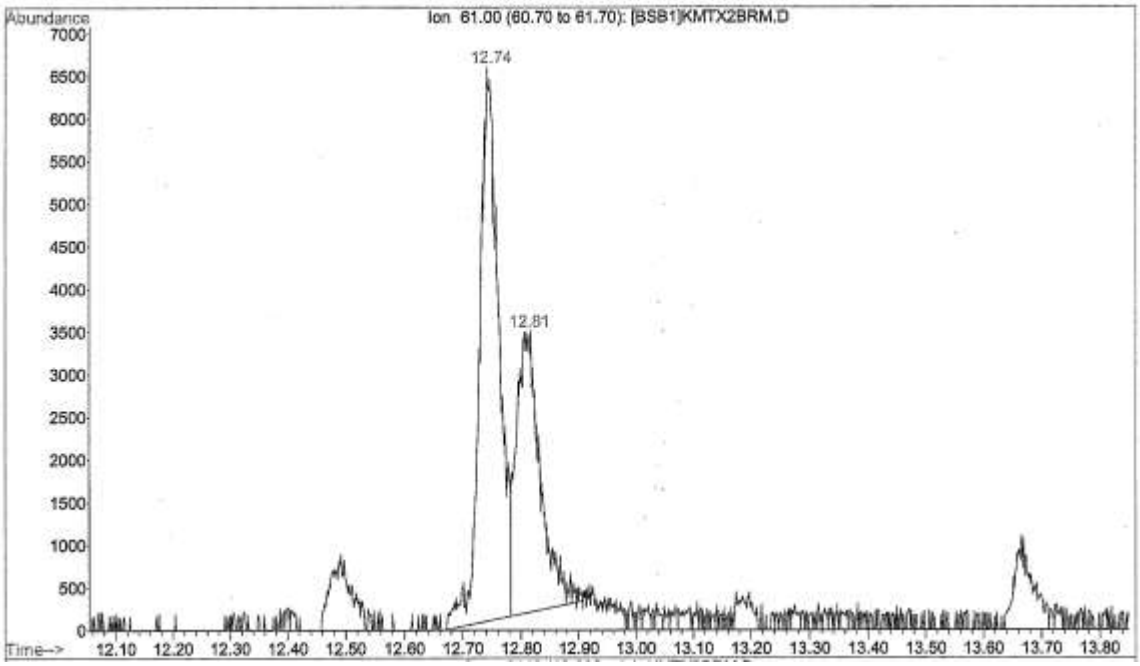

d. GC/MS of the mixture of KmTx2 Grubbs' metathesis products and (*S*)-Pent-4-ene-1,2-diol (**5b**)

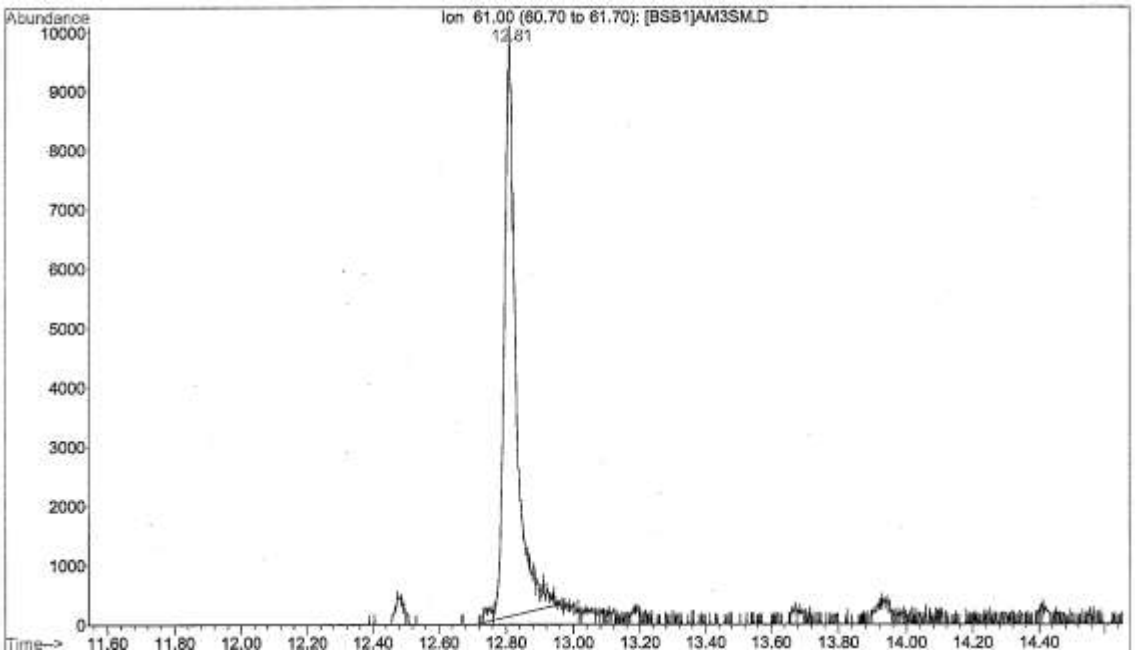

e. GC/MS of the mixture of amphidinol 3 Grubbs' metathesis products and (*R*)-Pent-4-ene-1,2-diol (**5a**)

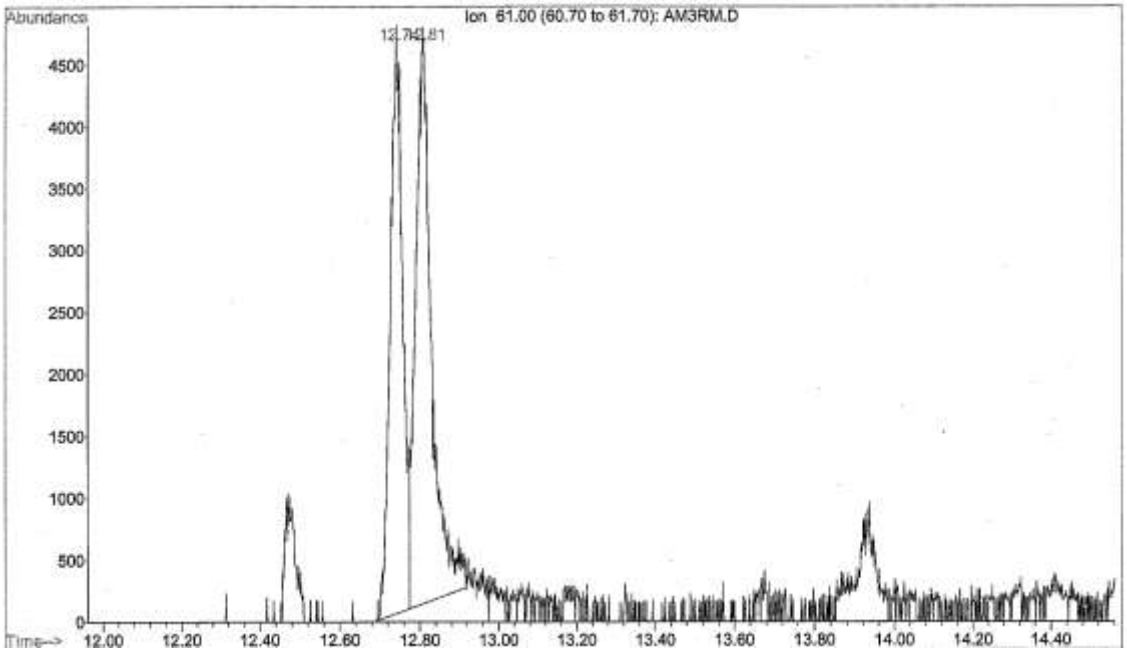

f. GC/MS of the mixture of amphidinol 3 Grubbs' metathesis products and (*S*)-Pent-4-ene-1,2-diol (**5b**)

Figure S16. GC/MS comparison of degradation **5c** with authentic **5b**/**5c**

3. Hemolytic Assay

The hemolytic assay performed using the HPLC fractions is described in detail elsewhere.[3] Briefly, rainbow trout (*Oncorhynchus mykis*) erythrocytes were extracted from the caudal vein and the blood washed three times with three volumes of buffer per mL of packed erythrocytes using the incubation buffer described below minus $CaCl_2$. Following the third wash the cells were resuspended in 3 mL of buffer per mL of packed cells. Resuspended cells were diluted 1:20 in buffer and 200 μL of diluted, washed erythrocytes were incubated in the presence of 10 μL of each HPLC fraction for 60 minutes in a buffer of 150 mM NaCl, 3.2 mM KCl, 1.25 mM $MgSO_4$, 12.2 mM Tris Base and 3.75 mM $CaCl_2$. Assays were run in 96 well, V-bottom, non-treated, polystyrene plates (Corning Inc.) sealed with Falcon 3073 pressure sensitive film (Becton Dickinson Labware). Assays were incubated on an orbital shaker (80-100 rpm) at 20 °C. Plates were then centrifuged at 2500 g for 5 min and the supernatant (100 μl) was transferred to a flat bottom 96 well polystyrene plate, where the absorbance of released hemoglobin was read at 540 nm using a microtiter plate spectrophotometer (Model Spectramax 340, Molecular Devices). Saponin (0-10 μg) (from *Quillaja* bark; Sigma Chemical Co.) was used as a positive hemolysin control.

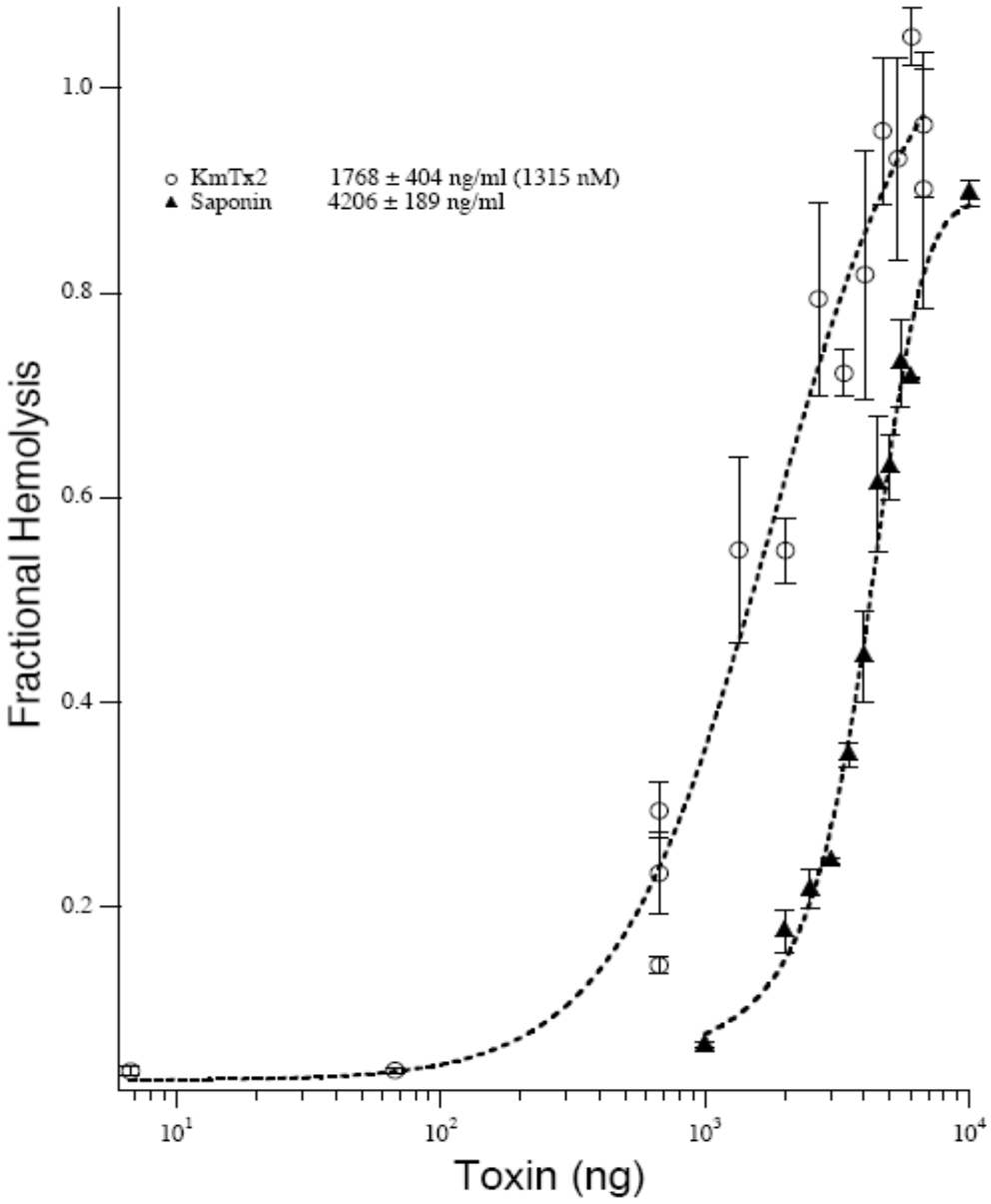

Figure S17. Relative hemolytic activity for KmTx 2 compared to saponin using Rainbow trout erythrocytes.

References

1. Andersen, R. A.; Morton, S. L.; Sexton, J. P. *J. Phycol.* **1997**, *33*, Supplement.
2. Daz, Y., Bravo, F., Castilln, S. *J. Org. Chem.*, **64**, 6508-6511 (1999).
3. Eschbach, E.; Scharsack, J.; John, U.; Medlin, L. *J. Appl. Toxicol.* **2001**, *21*, 513-539.

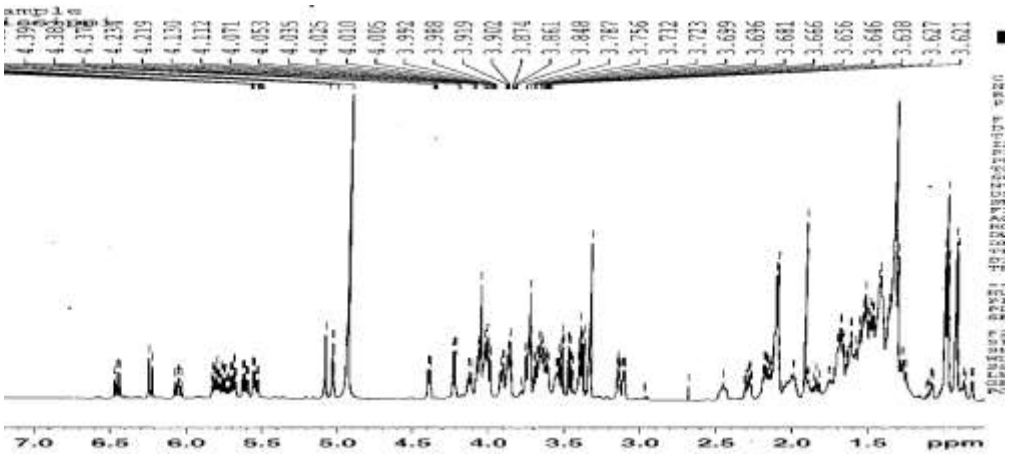
4.396
4.380
4.378
4.238
4.219
4.139
4.112
4.071
4.053
4.035
4.025
4.010
4.006
3.992
3.988
3.919
3.902
3.874
3.861
3.848
3.787
3.756
3.712
3.723
3.699
3.696
3.681
3.666
3.656
3.646
3.638
3.627
3.621
7.0
6.5
6.0
5.5
5.0
4.5
4.0
3.5
3.0
2.5
2.0
1.5
ppm

KTX 13C enriched sample
University of Mississippi
1D carbon spectrum, power gated

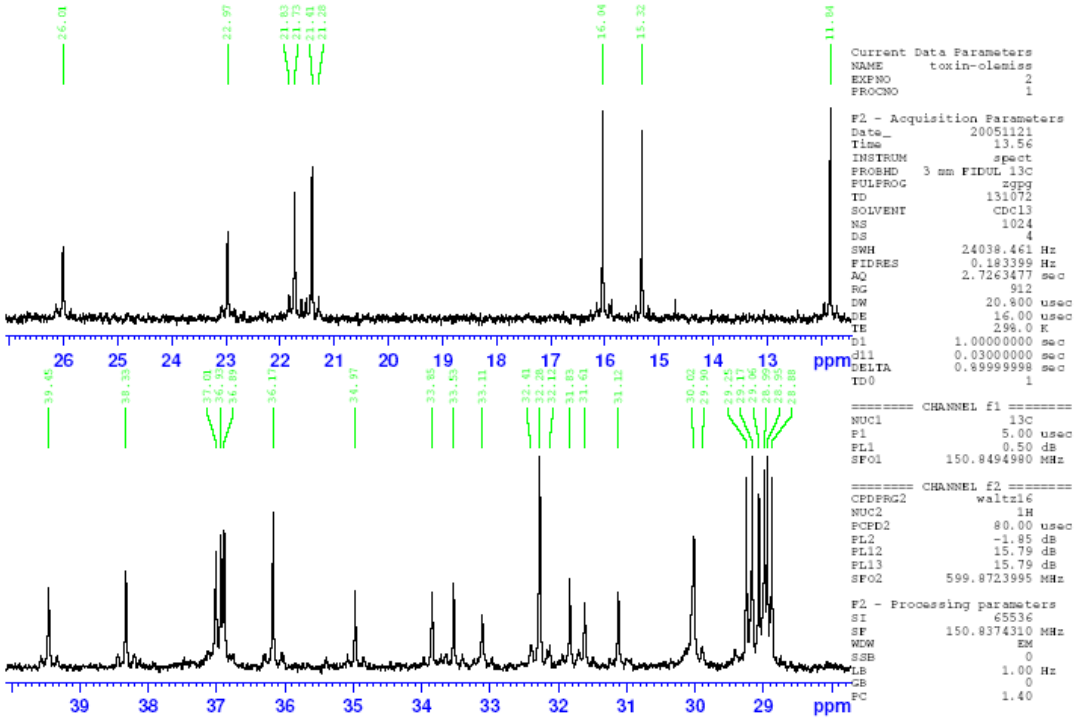

KTX 13C enriched sample
University of Mississippi
1D carbon spectrum, power gated

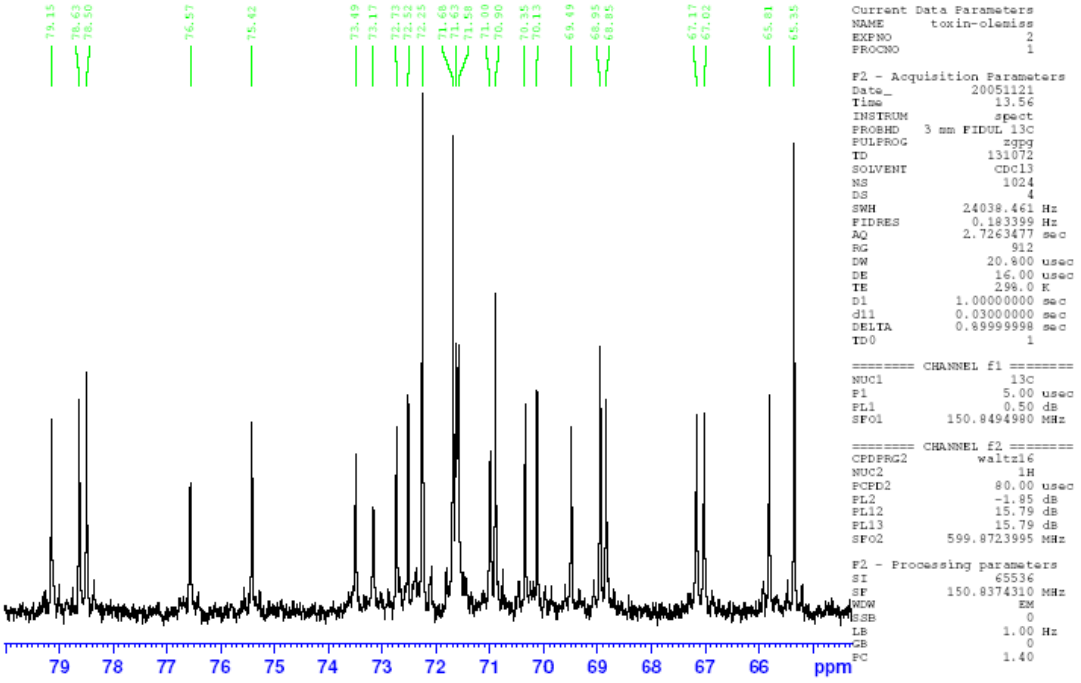

KTX 13C enriched sample
University of Mississippi
1D carbon spectrum, power gated

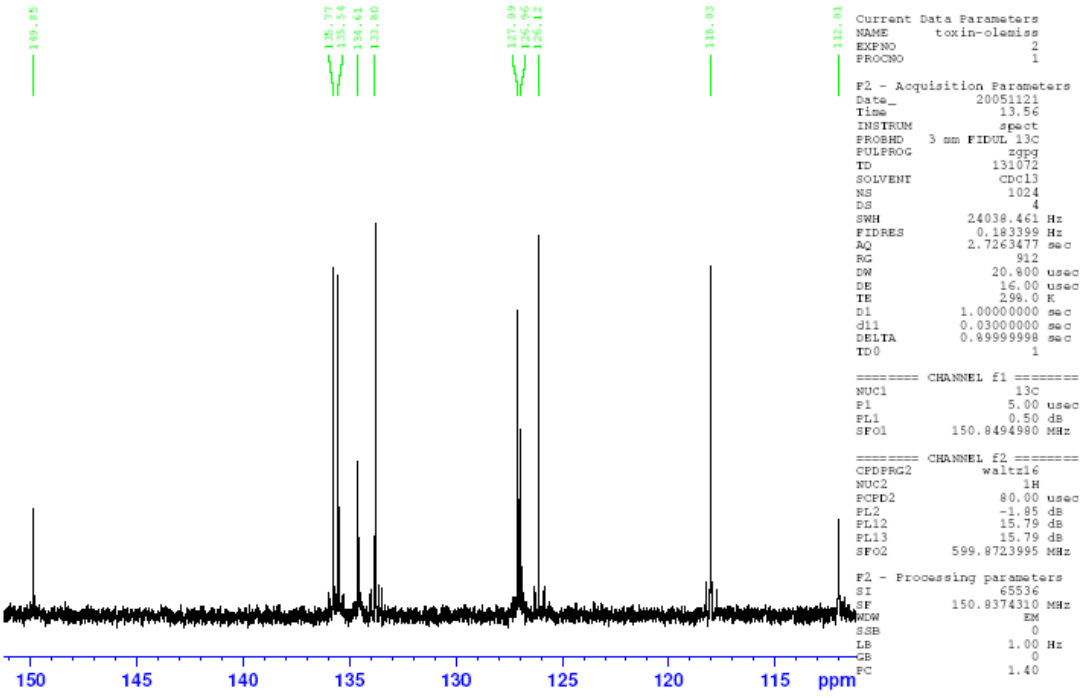

Current Data Parameters
NAME toxin-olamiss
EXPNO 2
PROCNO 1

F2 - Acquisition Parameters
Date_ 20051121
Time 13.56
INSTRUM spect
PROBHD 3 mm PIDUL 13C
PULPROG zgpg
TD 131072
SOLVENT CDCl3
NS 1024
DS 4
SWH 24038.461 Hz
FIDRES 0.183399 Hz
AQ 2.7263477 sec
RG 912
DW 20.800 usec
DE 16.00 usec
TE 298.0 K
D1 1.00000000 sec
d11 0.03000000 sec
DELTA 0.89999998 sec
TD0 1

======== CHANNEL f1 ========
NUC1 13C
P1 5.00 usec
PL1 0.50 dB
SFO1 150.8494980 MHz

======== CHANNEL f2 ========
CPDPRG2 waltz16
NUC2 1H
PCPD2 80.00 usec
PL2 -1.85 dB
PL12 15.79 dB
PL13 15.79 dB
SFO2 599.8723995 MHz

F2 - Processing parameters
SI 65536
SF 150.8374310 MHz
WDW EM
SSB 0
LB 1.00 Hz
GB 0
PC 1.40

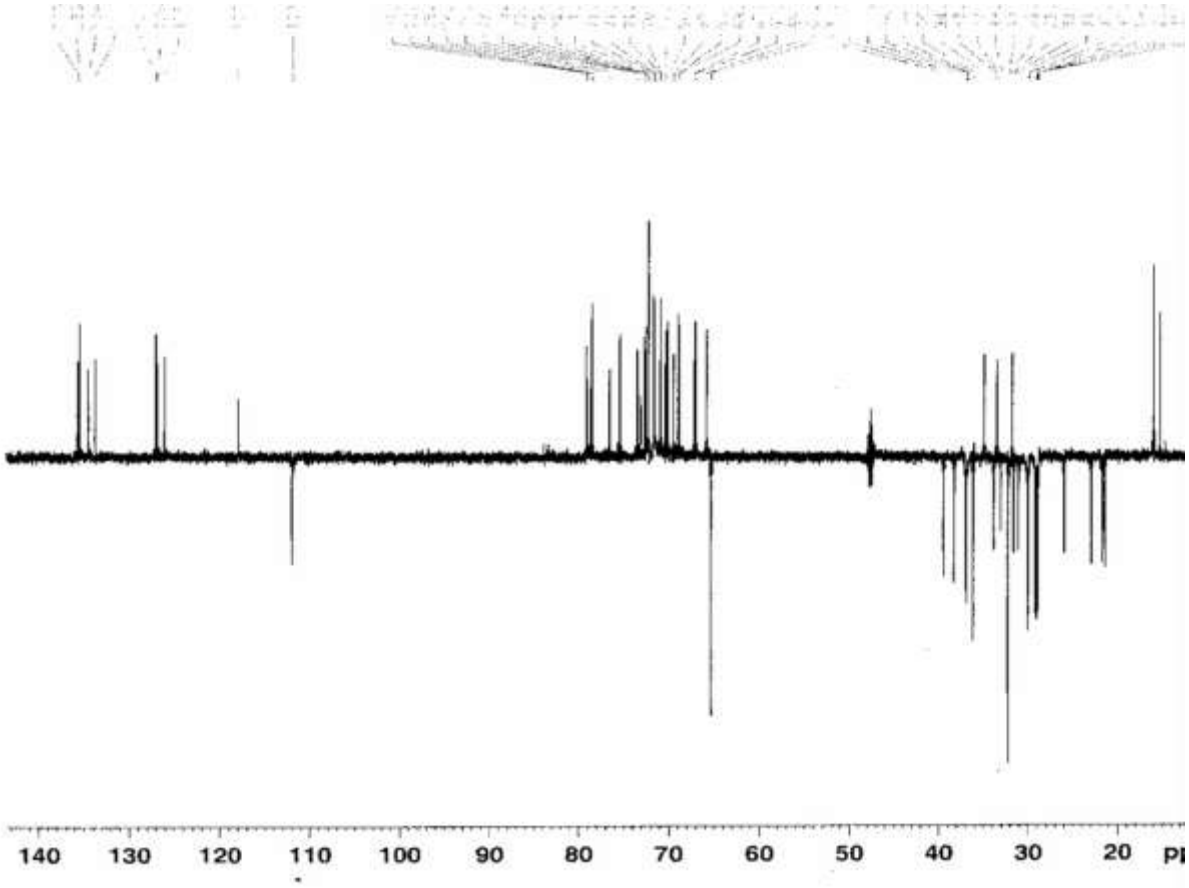
140
130
120
110
100
90
80
70
60
50
40
30
20

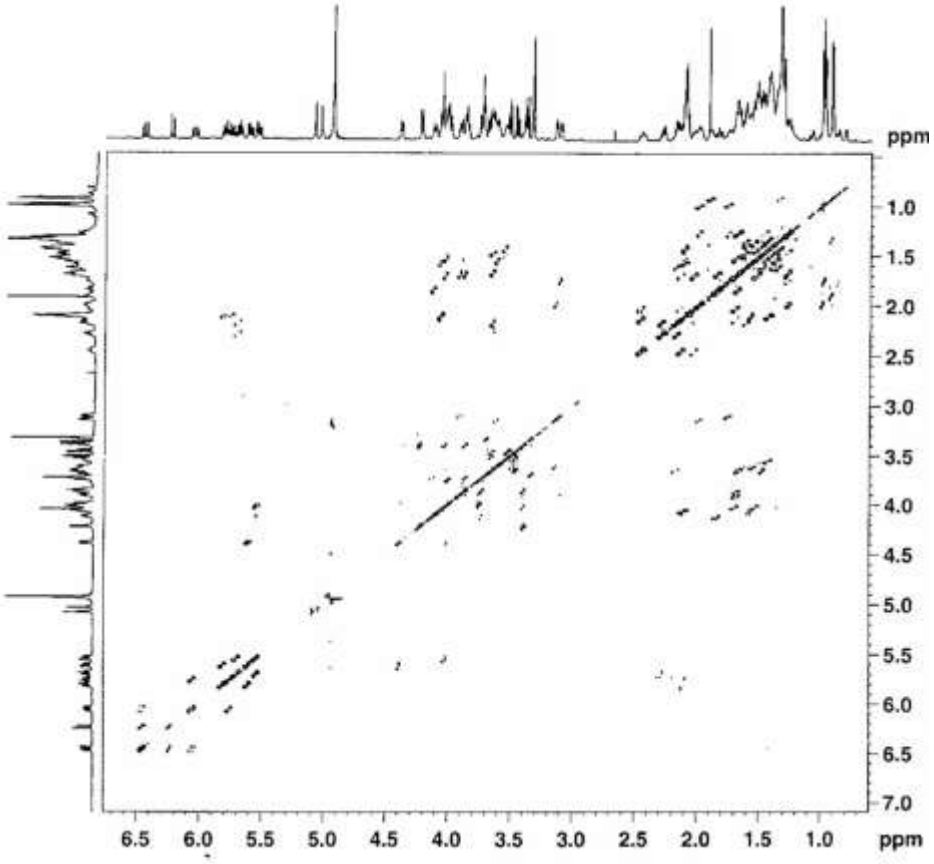

COSY Spectrum of Karlotoxin-2

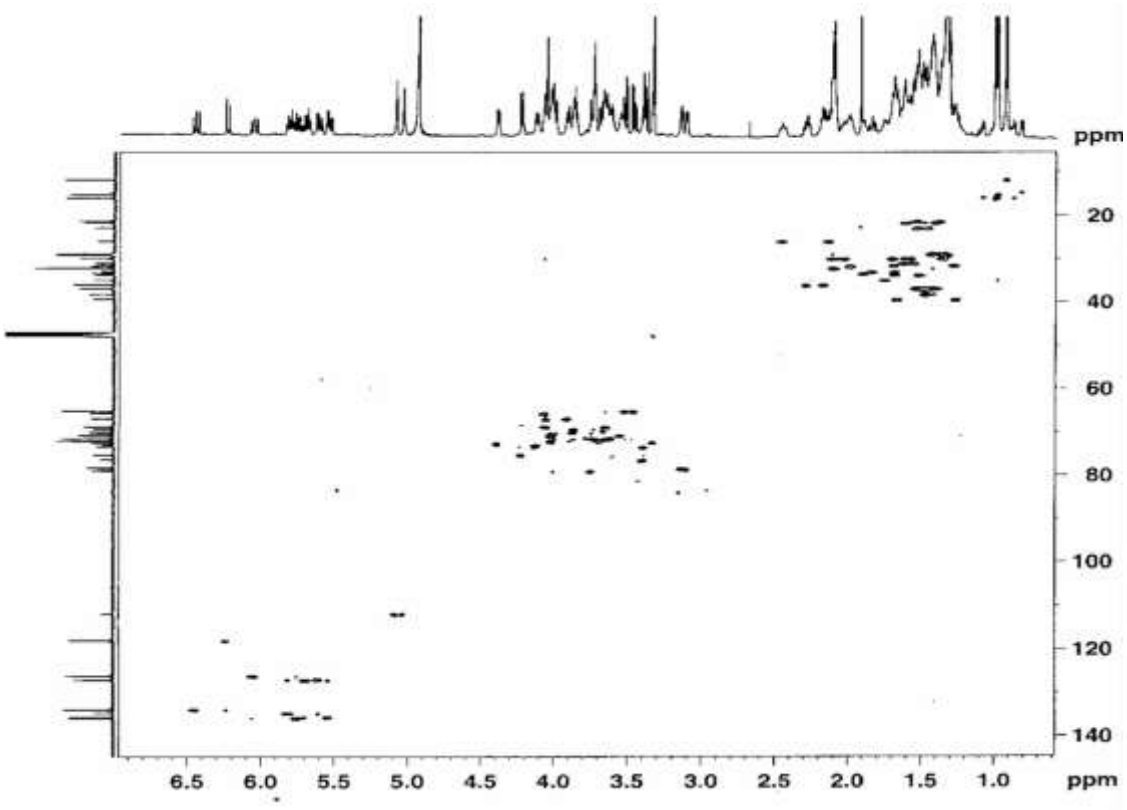

HMQC Spectrum of Karlotoxin-2

‘

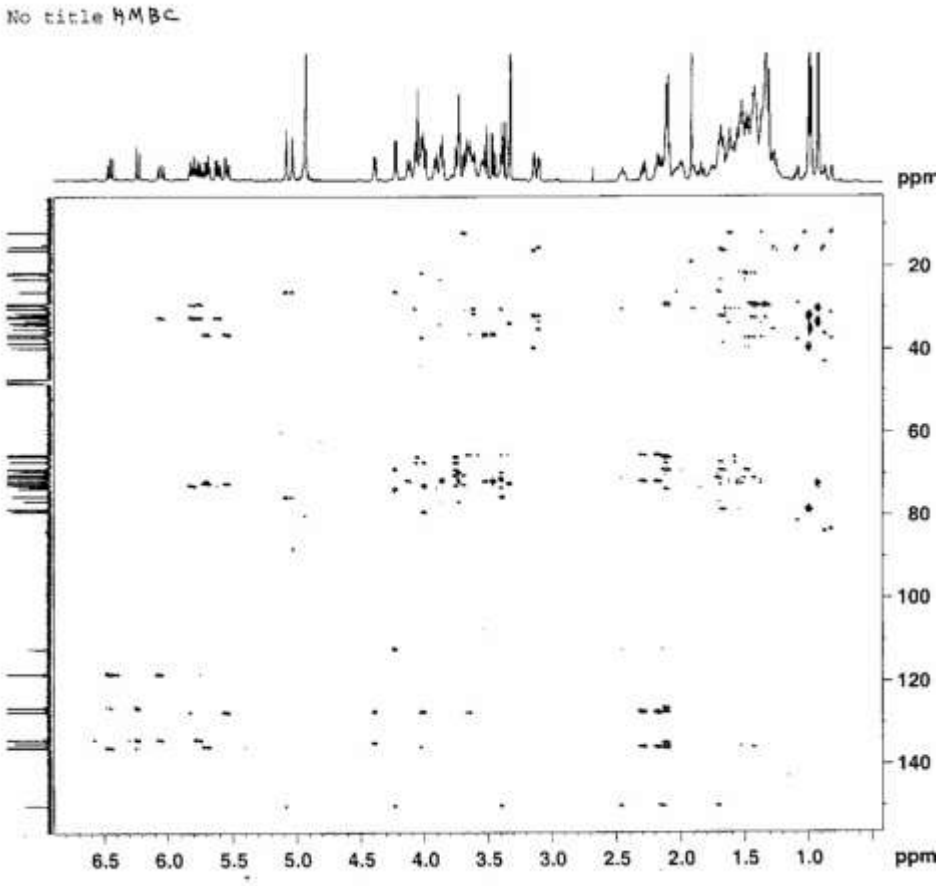

HMBC Spectrum of Karlotoxin-2

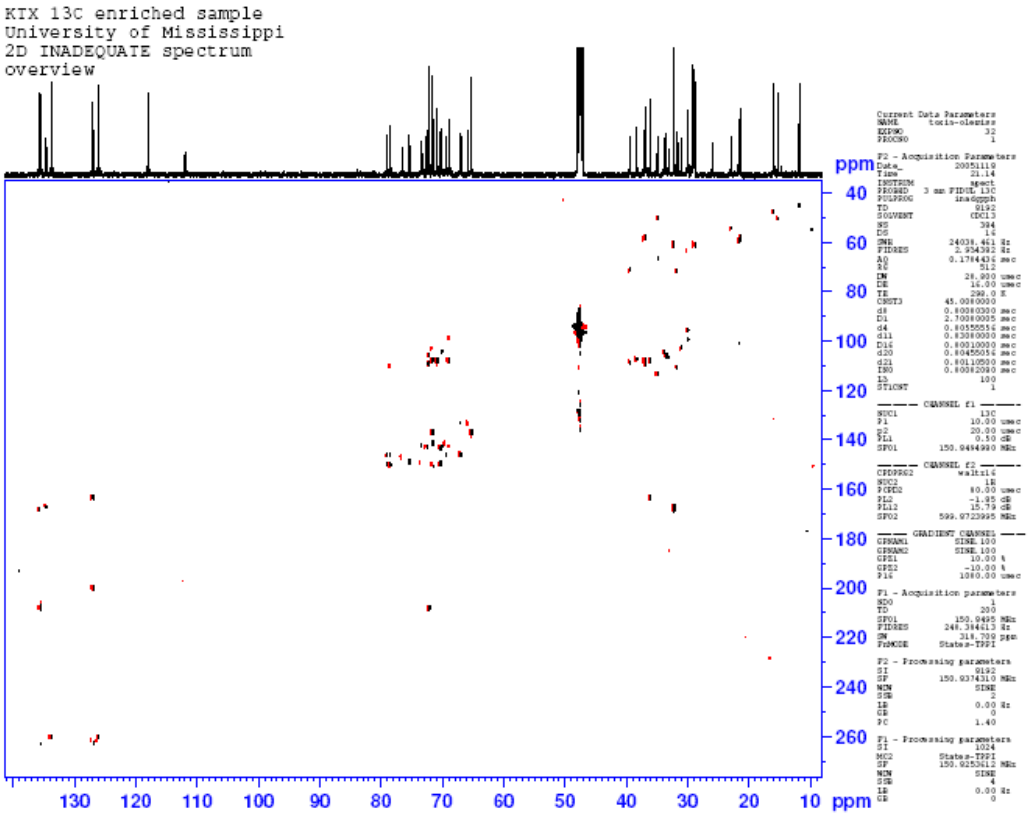

2D INADEQUATE of Karlotoxin-2

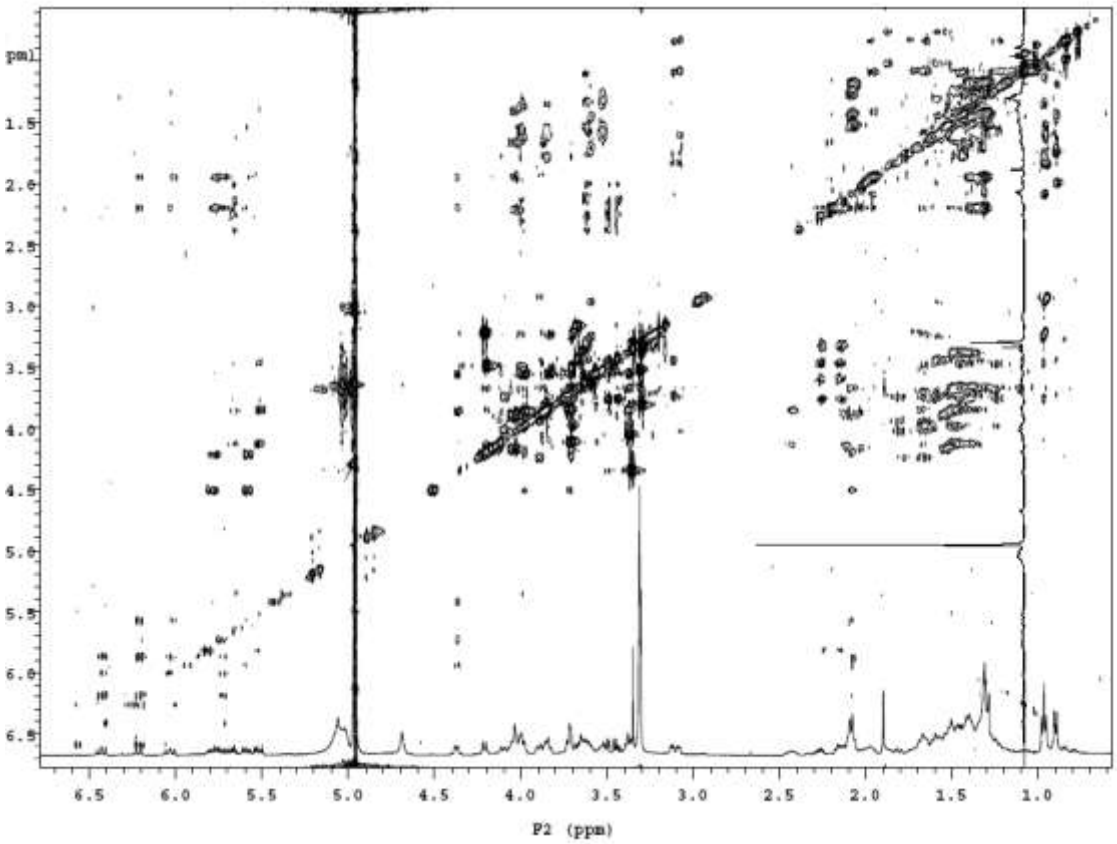

HETLOC Spectrum of Karlotoxin-2

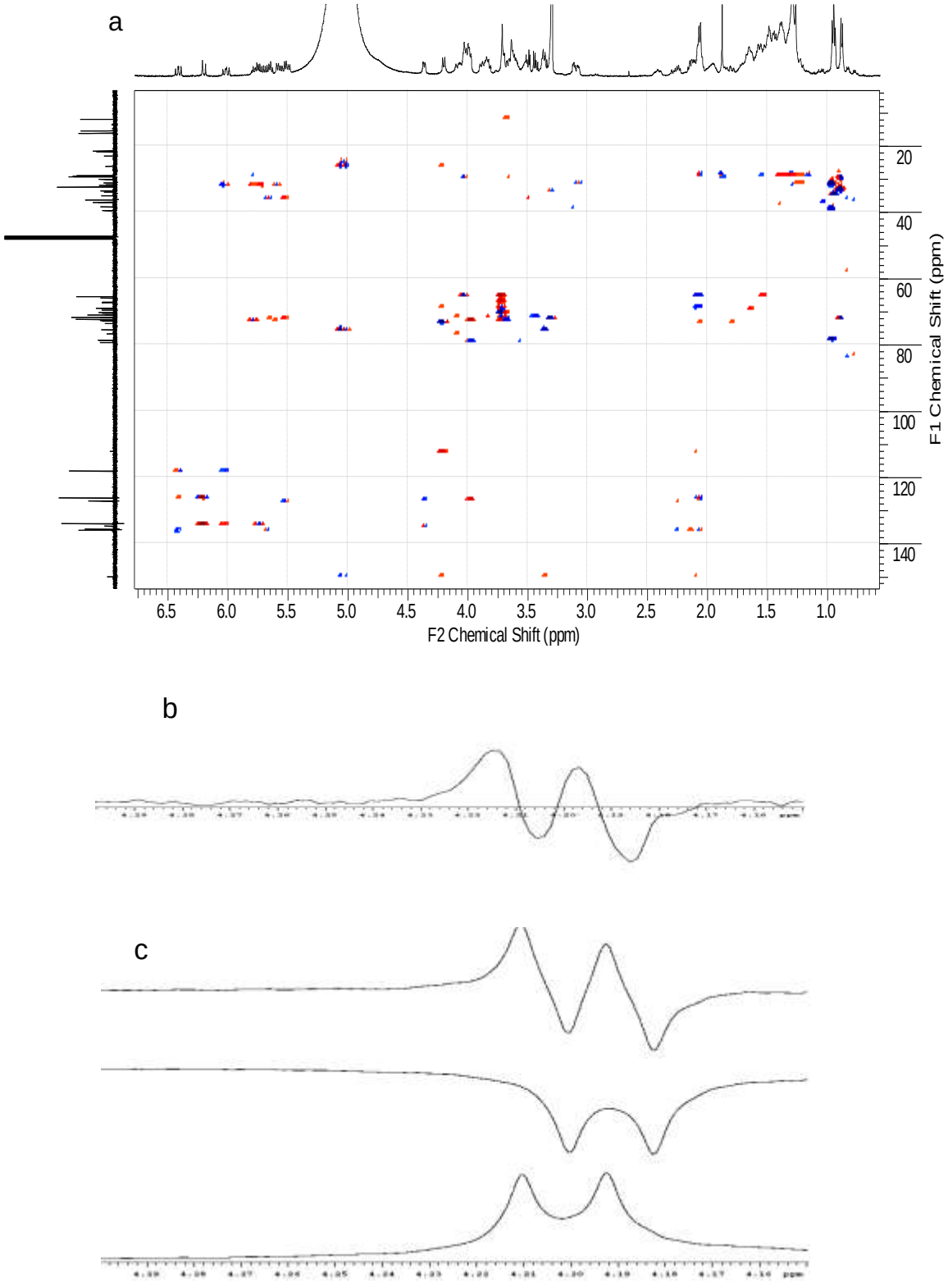

HSQMBC Spectrum of Karlotoxin-2: a. HSQMBC spectrum; b. slice from HSQMBC spectrum. c. mimic spectrum by adding proton spectra with a -5 Hz shift